Acta Mech 211, 181–193 (2010)
DOI 10.1007/s00707-009-0233-9

V. A. Osinov

Transition from acceleration waves to strong discontinuities in fluid-saturated solids: drained versus undrained behaviour

Received: 30 March 2009 / Revised: 14 August 2009 / Published online: 12 September 2009

Abstract The evolution of compression waves propagating in a fluid-saturated granular solid is considered. The pore fluid is assumed to consist of a liquid with a small amount of free gas. The stiffness of such a solid increases with increasing pressure. This property leads to the transformation of continuous compression waves into shock fronts after a finite time of propagation. The aim of the study is to calculate the critical distance covered by a continuous wave before it loses continuity. Critical distances are calculated for weak discontinuities (acceleration waves) propagating into a quiescent region. In numerical examples, the pressure dependence of the stiffness is taken in a form typical of granular solids. Emphasis is placed on the influence of free gas in the pore fluid and the permeability of the skeleton. Comparison of locally undrained and drained behaviour reveals that the drained model with low permeability turns out to be misleading for the calculation of the critical distance of a compression wave.

1 Introduction

The formation of strong discontinuities (shock fronts) from continuous compression waves propagating in gases has long been known and extensively studied [1]. The steepening of the profile of a compression front and the eventual transition to a shock front are consequences of the fact that the compressibility of gases decreases in compression. In comparison with gases, the stiffness of granular solids such as sand, soil or powders is a more complex tensorial quantity which depends on the stress state, the current and the foregoing deformation and other factors. However, a general property of granular solids is that their stiffness increases with increasing pressure. As in the case with gases, this property leads to the transformation of continuous compression waves into shock fronts and to the nonexistence of a classical (continuous) solution after a finite time of propagation.

The dependence of the stiffness on the confining pressure in granular materials is brought about by their granular structure. If a granular material is saturated with a fluid, the compressibility of the fluid may depend on its pressure and thus, apart from the properties of the solid skeleton, constitute another source of the pressure-dependent stiffness of the body. In particular, the compressibility of a pore fluid becomes pressure dependent if the fluid is not a pure liquid but a liquid with a small amount of free gas entrapped in the pore space.

A so-called critical distance which a continuous compression front covers before it loses continuity and turns into a shock front depends on the constitutive properties of the medium and on the rate of the boundary loading which induces the front. A higher rate results in a shorter critical distance. In applications, an estimation of the critical distance may be required in order to choose a proper computational technique for the solution of a dynamic boundary value problem of wave propagation. If the estimated critical distance is not larger than the size of the spatial domain in the problem under study, the numerical algorithm has to allow for

V. A. Osinov (✉)
Institute of Soil Mechanics and Rock Mechanics, University of Karlsruhe, 76128 Karlsruhe, Germany
E-mail: vladimir.osinov@ibf.uni-karlsruhe.de

solutions with strong discontinuities. For instance, in the context of soil dynamics, the rates of loading caused by an earthquake and an explosion differ by several orders of magnitude, and the same holds for the critical distances. Whereas the critical distance due to an earthquake may be large enough to neglect the formation of a shock front, the critical distance corresponding to a blast loading may be as short as a few centimetres and thus lie within the computational domain.

For solids with rate-independent constitutive behaviour, a plane compression front propagating into a quiescent region is a so-called simple wave [1]. Due to the special structure of such a solution, it is possible to calculate the evolution of the gradients of the solution in each point of a continuous wave profile and thus to find the critical distance for a wave profile of arbitrary shape [2]. For fluid-saturated porous solids, a compression front is a simple-wave solution if the relative motion between the solid and the fluid phases may be neglected due to the low permeability of the skeleton. If the permeability is not low enough and the dynamic problem has to be solved with locally drained conditions, the wave becomes dissipative and is no longer a simple wave. This fact does not allow us to derive a tractable equation for the evolution of the gradients on the wave profile in the drained case.

Rather than considering smooth wave fronts, the critical distances can alternatively be calculated from the evolution of weak discontinuities, i.e. jumps in the first partial derivatives of the solution. For a propagating weak discontinuity (acceleration wave), infinite growth of its amplitude in a finite time signifies the transition from the continuous solution to a strong discontinuity and the formation of a shock front. If a weak discontinuity propagates into a domain where the solution is known, the evolution equation for the amplitude of the discontinuity can be solved directly, and thus the critical distance can be found.

The objective of the present study is, using the acceleration-wave approach, to calculate the critical distances for plane compression fronts in a saturated granular solid and to compare the results for locally drained and undrained behaviour. To obtain the numerical estimations of the critical distances, the pressure dependence of the stiffness of the solid skeleton is taken in a particular form typical of granular skeletons. Emphasis is placed on the influence of the permeability of the skeleton and a small amount of free gas in the pore fluid.

A feature of the comparative analysis of undrained and drained behaviour is that the evolution equation for the amplitude of an acceleration wave in the drained case with low permeability leads to essentially different results as compared with purely undrained behaviour. This inconsistency stems from the fact that, as the permeability tends to zero, the dynamic equations in the drained case degenerate rather than reduce to the equations in the undrained case. In this connection, the question arises as to what model—with drained or undrained behaviour—should be used in applications at low permeability.

2 Evolution of weak discontinuities

Plane longitudinal waves in both drained and undrained cases considered in this paper are described by a system of equations in the form

$$\frac{\partial u_i}{\partial t} + A_{ij}(u_1, \ldots, u_N)\frac{\partial u_j}{\partial x} = B_i(u_1, \ldots, u_N), \quad i = 1, \ldots, N, \tag{1}$$

where $u_1, \ldots, u_N$ are unknown functions, and the variables x and t stand for a spatial coordinate and time, respectively. The coefficients of the system, A_{ij}, and the right-hand sides, B_i, are assumed to be functions of u_i with continuous first partial derivatives $\partial A_{ij}/\partial u_k$, $\partial B_i/\partial u_j$.

Given continuous initial and boundary data, the quasilinear system (1) may have a continuous solution only within a finite time [3]. For data with a weak discontinuity, the evolution of the amplitude of the discontinuity for system (1) is shown to be described by an ordinary differential equation of the Bernoulli type [4–9]. The coefficients of this equation can be expressed in different ways. We will use the evolution equation in the form derived in [8,9] (see equation (C.112) in [8] or (9) in [9] and details of the derivation therein).

A curve on which the first derivatives $\partial u_i/\partial x$, $\partial u_i/\partial t$ of a solution to (1) are discontinuous is necessarily a characteristic curve of system (1). The speed of propagation of the discontinuity front in space, c, is a (real) eigenvalue of the matrix A_{ij}. Let $[\![\ ]\!] = (\ )^+ - (\ )^-$ denote the jump of a quantity across the front, with $(\ )^+$ and $(\ )^-$ being the values ahead of and behind the front, respectively. The vector $[\![\partial u_i/\partial x]\!]$ is shown to be a right eigenvector of the matrix A_{ij} associated with the eigenvalue c. If the algebraic multiplicity of the considered eigenvalue c is equal to one, any discontinuity $[\![\partial u_i/\partial x]\!]$ can be represented as

$$\left[\!\left[\frac{\partial u_i}{\partial x}\right]\!\right] = aR_i, \quad i = 1, \ldots, N, \tag{2}$$

where R_i are the components of a right eigenvector of A_{ij} associated with the eigenvalue c, and a is a scalar factor subsequently referred to as the amplitude of the discontinuity.

The amplitude a as a function of time satisfies the equation

$$\frac{\mathrm{d}a}{\mathrm{d}t} + \alpha_1 a + \alpha_2 a^2 = 0, \tag{3}$$

where the coefficients are given by Wilmanski [8,9]

$$\alpha_1 = \frac{L_i}{R_k L_k}\left[R_l \frac{\partial A_{ij}}{\partial u_l}\left(\frac{\partial u_j}{\partial x}\right)^+ + R_j \frac{\partial A_{ij}}{\partial u_l}\left(\frac{\partial u_l}{\partial x}\right)^+ - R_j \frac{\partial B_i}{\partial u_j} + \frac{\mathrm{d}R_i}{\mathrm{d}t}\right], \tag{4}$$

$$\alpha_2 = -\frac{L_i R_j R_l}{R_k L_k}\frac{\partial A_{ij}}{\partial u_l}. \tag{5}$$

In (4) and (5), L_i are the components of a left eigenvector of A_{ij} associated with the eigenvalue c, and $\mathrm{d}R_i/\mathrm{d}t$ is the time derivative of R_i along the characteristic.

Since a, α_1, α_2 are specified on a characteristic curve, they can be viewed as functions of either t or x. In the latter case, replacing the temporal derivative along the characteristic with the spatial one, $\mathrm{d}(\,)/\mathrm{d}t = c\,\mathrm{d}(\,)/\mathrm{d}x$, we can rewrite the evolution equation (3) in terms of x:

$$c\frac{\mathrm{d}a}{\mathrm{d}x} + \alpha_1 a + \alpha_2 a^2 = 0. \tag{6}$$

If the discontinuity front propagates into a region where the functions u_i are known, the coefficients α_1, α_2 and c in (6) become known functions of x. Equation (6) with known coefficients is the Bernoulli equation which can be solved for $a(x)$. The solution is

$$a(x) = \left(\frac{1}{a_0} + \int_{x_0}^{x} \frac{\alpha_2 \psi}{c}\mathrm{d}\xi\right)^{-1} \psi(x), \tag{7}$$

where

$$\psi(x) = \exp\left(-\int_{x_0}^{x} \frac{\alpha_1}{c}\mathrm{d}\eta\right), \tag{8}$$

and a_0 is the initial amplitude at $x = x_0$. It is seen from (7) that, if α_2 is not identically zero, (6) may possess solutions which become infinite at a finite x. The critical distance x_c is found from the equation

$$\frac{1}{a_0} + \int_{x_0}^{x_0+x_\mathrm{c}} \frac{\alpha_2 \psi}{c}\mathrm{d}\xi = 0. \tag{9}$$

The condition that α_2 must be nonzero for the critical distance to be finite means that some coefficients A_{ij} of system (1) must be functions of u_i, see (5), and, hence, the system must be nonlinear.

In what follows we will deal with the special cases where α_1 and α_2 are constants. In turn, α_1 may be zero or not. If $\alpha_1 = 0$, the solution to (9) is

$$x_\mathrm{c} = -\frac{c}{\alpha_2 a_0}. \tag{10}$$

If $\alpha_1 \neq 0$, the critical distance is given by

$$x_\mathrm{c} = -\frac{c}{\alpha_1}\ln\left(1 + \frac{\alpha_1}{\alpha_2 a_0}\right). \tag{11}$$

A solution x_c to (9) and, in particular, solutions given by (10) and (11) are physically relevant if their sign coincides with the sign of c. Besides the critical distance, Eqs. (10) and (11) determine the range of initial amplitudes a_0 for which a finite critical distance with a proper sign exists.

3 Undrained behaviour

The total stress in a porous solid saturated with a fluid can be decomposed into the effective stress in the skeleton and an isotropic stress due to the fluid pressure:

$$\boldsymbol{\sigma}_{\text{total}} = \boldsymbol{\sigma} - p\,\mathbf{I}, \tag{12}$$

where $\boldsymbol{\sigma}_{\text{total}}$ and $\boldsymbol{\sigma}$ are, respectively, the total and the effective stress tensors (compressive stresses are negative), p is the fluid pressure (positive for compression), and $\mathbf{I}$ is the unit tensor. The decomposition (12) is justified if the compressibility of the skeleton is much higher than that of the solid phase [10]. This holds, in particular, for soils. According to the effective-stress principle, the constitutive equation for the effective stress tensor in a saturated solid is independent of the pore pressure and is the same as for the dry skeleton.

Introduce a rectangular Cartesian coordinate system (x_1, x_2, x_3) and consider plane longitudinal waves propagating along the x_1-axis with one nonzero velocity component v_1 and three nonzero stress components $\sigma_{11}, \sigma_{22}, \sigma_{33}$. For brevity, in the equations below we will write $\sigma_1, \sigma_2, \sigma_3, v, x$ for $\sigma_{11}, \sigma_{22}, \sigma_{33}, v_1, x_1$, respectively.

In the absence of the relative motion between the solid and the fluid phases and without mass forces, the equation of motion for longitudinal waves is

$$\frac{\partial v}{\partial t} - \frac{1}{\varrho}\frac{\partial \sigma_1}{\partial x} + \frac{1}{\varrho}\frac{\partial p}{\partial x} = 0, \tag{13}$$

where $\varrho = n\varrho_{\text{f}} + (1-n)\varrho_{\text{s}}$ is the mean density, ϱ_{f} and ϱ_{s} are the densities of the fluid and the solid constituents, and n is the porosity of the skeleton. In the governing equations in this paper, the convective terms in the material time derivatives are neglected, and the material derivatives are replaced with the partial ones. The constitutive equations for the effective stresses are written in rate form and are taken to be incrementally linear:

$$\frac{\partial \sigma_1}{\partial t} - \kappa_1 \frac{\partial v}{\partial x} = 0, \tag{14}$$

$$\frac{\partial \sigma_2}{\partial t} - \kappa_2 \frac{\partial v}{\partial x} = 0, \tag{15}$$

$$\frac{\partial \sigma_3}{\partial t} - \kappa_3 \frac{\partial v}{\partial x} = 0, \tag{16}$$

where the stiffness coefficients $\kappa_1, \kappa_2, \kappa_3$ are functions of the current principal stresses $\sigma_1, \sigma_2, \sigma_3$. Under locally undrained conditions, the evolution of the pore pressure is governed by the equation

$$\frac{\partial p}{\partial t} + \frac{K_{\text{f}}}{n}\frac{\partial v}{\partial x} = 0, \tag{17}$$

where the compression modulus of the pore fluid, K_{f}, may be a function of the fluid pressure p.

System (13)–(17) is of the form (1) with

$$u_1 = v, \quad u_2 = \sigma_1, \quad u_3 = \sigma_2, \quad u_4 = \sigma_3, \quad u_5 = p. \tag{18}$$

The calculation of the eigenvalues of the matrix A_{ij} for system (13)–(17) gives three zero eigenvalues and two eigenvalues $\pm c_{\text{u}}$ with

$$c_{\text{u}} = \sqrt{\frac{1}{\varrho}\left(\kappa_1 + \frac{K_{\text{f}}}{n}\right)}, \tag{19}$$

where the notation c_{u} is used for the positive characteristic wave speed in the undrained case. The components of the right and the left eigenvectors of the matrix A_{ij} associated with the eigenvalue c_{u} are

$$R_2 = -\frac{\kappa_1}{c_{\text{u}}}R_1, \quad R_3 = -\frac{\kappa_2}{c_{\text{u}}}R_1, \quad R_4 = -\frac{\kappa_3}{c_{\text{u}}}R_1, \quad R_5 = \frac{K_{\text{f}}}{nc_{\text{u}}}R_1, \tag{20}$$

$$L_2 = -\frac{1}{\varrho c_{\text{u}}}L_1, \quad L_3 = 0, \quad L_4 = 0, \quad L_5 = \frac{1}{\varrho c_{\text{u}}}L_1, \tag{21}$$

where R_1, L_1 are arbitrary. From (20), (21) we obtain the scalar product of the two eigenvectors: $R_i L_i = 2R_1 L_1$.

We will consider the propagation of a weak discontinuity with the positive speed c_u into a quiescent region where $v = 0$ and $\sigma_1, \sigma_2, \sigma_3, p$ do not depend on x and t. The density and the porosity are assumed to be homogeneous. In this case the first two terms on the right-hand side of (4) vanish. The third term vanishes as well because $B_i = 0$ in (13)–(17). Since all quantities ahead of the wave front are homogeneous and, hence, the components of the matrix A_{ij} are constant on the front, we can always take the same right eigenvector and thus have $\mathrm{d}R_i/\mathrm{d}t = 0$ in (4). This gives $\alpha_1 = 0$. Calculating the derivatives $\partial A_{ij}/\partial u_l$ involved in (5) (with the density and the porosity treated as constants), we obtain

$$\alpha_2 = \frac{R_1 \beta}{2\varrho c_\mathrm{u}^2}, \tag{22}$$

where

$$\beta = \kappa_1 \frac{\partial \kappa_1}{\partial \sigma_1} + \kappa_2 \frac{\partial \kappa_1}{\partial \sigma_2} + \kappa_3 \frac{\partial \kappa_1}{\partial \sigma_3} - \frac{K_\mathrm{f}}{n^2} \frac{\mathrm{d}K_\mathrm{f}}{\mathrm{d}p}. \tag{23}$$

In order to calculate the critical distance from Eq. (9), it is necessary to specify the initial amplitude of the discontinuity, a_0, at the boundary $x = x_0$ at $t = 0$. We consider a boundary value problem in which the total stress $\sigma_1 - p$ is prescribed at the boundary:

$$\sigma_1(x_0, t) - p(x_0, t) = f(t), \quad t \geq 0, \tag{24}$$

where $f(t)$ is a given function, and $f(0)$ is equal to the initial total stress in the domain $x \geq x_0$. Let s_0 denote the initial rate of $f(t)$ at $t = 0$:

$$s_0 = \left. \frac{\mathrm{d}f}{\mathrm{d}t} \right|_{t=0}. \tag{25}$$

At the beginning of the propagation at an infinitesimally small time Δt, the incipient spatial profile of the total stress $\sigma_1(x) - p(x)$ is linear. The initial gradient of the total stress behind the front produced by the rate s_0 in the immediate vicinity of x_0 is $-s_0 \Delta t/\Delta x$, where $\Delta x = c_\mathrm{u} \Delta t$ is the distance travelled by the wave front. This gives

$$\left(\frac{\partial \sigma_1}{\partial x}\right)^- - \left(\frac{\partial p}{\partial x}\right)^- = -\frac{s_0}{c_\mathrm{u}}. \tag{26}$$

On the other hand, the jumps $[\![\partial \sigma_1/\partial x]\!]$, $[\![\partial p/\partial x]\!]$ are proportional to the corresponding components of the right eigenvector of A_{ij}, see (2), that is,

$$\left[\!\left[\frac{\partial \sigma_1}{\partial x}\right]\!\right] = -\left(\frac{\partial \sigma_1}{\partial x}\right)^- = a_0 R_2, \tag{27}$$

$$\left[\!\left[\frac{\partial p}{\partial x}\right]\!\right] = -\left(\frac{\partial p}{\partial x}\right)^- = a_0 R_5. \tag{28}$$

Substituting (27), (28) into (26) and using (19), (20), we obtain for the initial amplitude:

$$a_0 = -\frac{s_0}{R_1 \varrho c_\mathrm{u}^2}. \tag{29}$$

Equation (10) then gives

$$x_\mathrm{c} = \frac{2\varrho^2 c_\mathrm{u}^5}{s_0 \beta}. \tag{30}$$

Since Eq. (30) is derived for a positive c_u, only a positive x_c has a physical meaning. This places a constraint on the sign of the boundary stress rate s_0. If the stiffness of the skeleton and the compression modulus of the pore fluid increase in compression, then β given by (23) is negative, so that s_0 must be negative as well. This is in accordance with the fact that only compression fronts turn into shock fronts.

4 Drained behaviour

If the relative motion between the fluid and the solid phases is taken into account, the equations of motion are written separately for each phase [10,11]:

$$\frac{\partial v_\mathrm{s}}{\partial t} - \frac{1}{(1-n)\varrho_\mathrm{s}}\frac{\partial \sigma_1}{\partial x} + \frac{1}{\varrho_\mathrm{s}}\frac{\partial p}{\partial x} = \frac{\varrho_\mathrm{f} g n^2}{(1-n)\varrho_\mathrm{s} k}(v_\mathrm{f} - v_\mathrm{s}), \tag{31}$$

$$\frac{\partial v_\mathrm{f}}{\partial t} + \frac{1}{\varrho_\mathrm{f}}\frac{\partial p}{\partial x} = -\frac{gn}{k}(v_\mathrm{f} - v_\mathrm{s}), \tag{32}$$

where v_s, v_f are the velocities of the solid and the fluid phases, respectively, k is the permeability of the skeleton (m/s), and g is the acceleration due to gravity. The constitutive equations for the effective stresses, (14)–(16), are now written in terms of the velocity of the skeleton:

$$\frac{\partial \sigma_1}{\partial t} - \kappa_1 \frac{\partial v_\mathrm{s}}{\partial x} = 0, \tag{33}$$

$$\frac{\partial \sigma_2}{\partial t} - \kappa_2 \frac{\partial v_\mathrm{s}}{\partial x} = 0, \tag{34}$$

$$\frac{\partial \sigma_3}{\partial t} - \kappa_3 \frac{\partial v_\mathrm{s}}{\partial x} = 0. \tag{35}$$

The generalised form of the constitutive equation (17) for the fluid pressure in the presence of seepage is

$$\frac{\partial p}{\partial t} + K_\mathrm{f}\left(\frac{1-n}{n}\right)\frac{\partial v_\mathrm{s}}{\partial x} + K_\mathrm{f}\frac{\partial v_\mathrm{f}}{\partial x} = 0. \tag{36}$$

System (31)–(36) is of the form (1) with

$$u_1 = v_\mathrm{s}, \quad u_2 = v_\mathrm{f}, \quad u_3 = \sigma_1, \quad u_4 = \sigma_2, \quad u_5 = \sigma_3, \quad u_6 = p. \tag{37}$$

For subsequent computations it is convenient to introduce the quantities

$$c_\mathrm{s} = \sqrt{\frac{\kappa_1}{(1-n)\varrho_\mathrm{s}}}, \quad c_\mathrm{f} = \sqrt{\frac{K_\mathrm{f}}{\varrho_\mathrm{f}}}, \tag{38}$$

which are the speeds of longitudinal waves in a dry skeleton and in the pore fluid, respectively, considered as individual continua.

We will use the notation c_d for the characteristic wave speeds in the drained case described by system (31)–(36). The calculation of the eigenvalues of the matrix A_{ij} for system (31)–(36) gives two zero eigenvalues and four eigenvalues as the roots of a second-order polynomial in c_d^2:

$$c_\mathrm{d}^4 - c_\mathrm{d}^2\left(c_\mathrm{s}^2 + c_\mathrm{f}^2\frac{(1-n)\varrho_\mathrm{f} + n\varrho_\mathrm{s}}{n\varrho_\mathrm{s}}\right) + c_\mathrm{s}^2 c_\mathrm{f}^2 = 0. \tag{39}$$

Four roots of (39) are $\pm c_{\mathrm{d}1}, \pm c_{\mathrm{d}2}$, where the notations $c_{\mathrm{d}1}, c_{\mathrm{d}2}$ are introduced for the positive wave speeds ordered so that $c_{\mathrm{d}1} > c_{\mathrm{d}2}$. It can be shown that $c_{\mathrm{d}1}, c_{\mathrm{d}2}$ satisfy the inequalities

$$c_{\mathrm{d}2} < c_\mathrm{s} < c_{\mathrm{d}1}, \quad c_{\mathrm{d}2} < c_\mathrm{f} < c_{\mathrm{d}1}. \tag{40}$$

The components of the right and the left eigenvectors of the matrix A_{ij} associated with a nonzero eigenvalue c_d are

$$R_2 = \frac{\varrho_\mathrm{s}}{\varrho_\mathrm{f}}\left(1 - \frac{c_\mathrm{s}^2}{c_\mathrm{d}^2}\right)R_1, \quad R_3 = -\frac{\kappa_1}{c_\mathrm{d}}R_1, \quad R_4 = -\frac{\kappa_2}{c_\mathrm{d}}R_1, \tag{41}$$

$$R_5 = -\frac{\kappa_3}{c_\mathrm{d}}R_1, \quad R_6 = \varrho_\mathrm{s}\left(c_\mathrm{d} - \frac{c_\mathrm{s}^2}{c_\mathrm{d}}\right)R_1, \tag{42}$$

$$L_2 = \frac{n(c_\mathrm{d}^2 - c_\mathrm{s}^2)}{(1-n)c_\mathrm{d}^2}L_1, \quad L_3 = -\frac{1}{(1-n)\varrho_\mathrm{s} c_\mathrm{d}}L_1, \tag{43}$$

$$L_4 = 0, \quad L_5 = 0, \quad L_6 = \frac{c_\mathrm{d}}{\varrho_\mathrm{s}(c_\mathrm{d}^2 - c_\mathrm{f}^2)}L_1, \tag{44}$$

where R_1, L_1 are arbitrary. From (41) to (44) we obtain

$$R_i L_i = \frac{2(c_{\mathrm{d}}^4 - c_{\mathrm{s}}^2 c_{\mathrm{f}}^2)}{c_{\mathrm{d}}^2 (c_{\mathrm{d}}^2 - c_{\mathrm{f}}^2)} R_1 L_1. \tag{45}$$

In the derivation of (45) and below, the ratio $\varrho_{\mathrm{f}}/\varrho_{\mathrm{s}}$ is eliminated with the help of the characteristic equation (39).

Consider a weak discontinuity propagating with the speed $c_{\mathrm{d}1}$ into a quiescent region where the stresses and the pore pressure are homogeneous. The first two terms on the right-hand side of (4) then vanish. Taking always the same right eigenvector on the wave front, we have $\mathrm{d}R_i/\mathrm{d}t = 0$. As distinct from the undrained case, the right-hand side of system (31)–(36) is nonzero and makes α_1 nonzero as well. The calculation of the required derivatives $\partial B_i/\partial u_j$ in (4) leads to

$$\alpha_1 = \frac{gn(c_{\mathrm{d}1}^2 - c_{\mathrm{s}}^2)(c_{\mathrm{f}}^2 - nc_{\mathrm{d}1}^2)^2}{2k(1-n)^2 c_{\mathrm{f}}^2 (c_{\mathrm{d}1}^4 - c_{\mathrm{s}}^2 c_{\mathrm{f}}^2)}. \tag{46}$$

Calculating the derivatives $\partial A_{ij}/\partial u_l$ for system (31)–(36) and inserting them into (5), we obtain

$$\alpha_2 = \frac{R_1(c_{\mathrm{d}1}^2 - c_{\mathrm{s}}^2)}{2(c_{\mathrm{d}1}^4 - c_{\mathrm{s}}^2 c_{\mathrm{f}}^2)} \left[\frac{\beta_1 c_{\mathrm{s}}^2 (c_{\mathrm{d}1}^2 - c_{\mathrm{f}}^2)}{c_{\mathrm{d}1}^2 - c_{\mathrm{s}}^2} - \frac{\mathrm{d}K_{\mathrm{f}}}{\mathrm{d}p} \frac{(1-n)c_{\mathrm{d}1}^4}{n(c_{\mathrm{d}1}^2 - c_{\mathrm{f}}^2)} \right], \tag{47}$$

where

$$\beta_1 = \frac{\partial \kappa_1}{\partial \sigma_1} + \frac{\kappa_2}{\kappa_1} \frac{\partial \kappa_1}{\partial \sigma_2} + \frac{\kappa_3}{\kappa_1} \frac{\partial \kappa_1}{\partial \sigma_3}. \tag{48}$$

A propagating weak discontinuity is assumed to be induced by a change in the total stress prescribed at the boundary $x = x_0$ as a function of time, see (24). In addition, the boundary is taken to be impermeable, which gives $v_{\mathrm{f}} = v_{\mathrm{s}}$ as a second boundary condition required for the drained problem. These two boundary conditions are consistent with the undrained case in the sense that, as the permeability tends to zero, the drained solution tends to the undrained one.

The calculation of the initial amplitude of the discontinuity, a_0, from a given boundary stress rate s_0 is now not as straightforward as in the undrained case. As distinguished from the undrained case where there is only one characteristic with a positive slope, now we have two ingoing characteristics with positive slopes, and the boundary rate s_0 induces simultaneously two weak discontinuities which travel with the speeds $c_{\mathrm{d}1}$ and $c_{\mathrm{d}2}$. As a consequence, the incipient wave profile at an infinitesimally small time is not linear but piecewise-linear and consists of two straight segments. The required relation between s_0 and a_0 is more complicated than in the undrained case. This relation can be found taking into account the second discontinuity propagating with the speed $c_{\mathrm{d}2}$ and the additional boundary condition $v_{\mathrm{f}} = v_{\mathrm{s}}$.

Numerical calculations performed with the particular constitutive equations adopted below for the solid skeleton and the pore fluid reveal that the critical distances obtained with the exact relation between s_0 and a_0 are very close to those obtained on the assumption that the incipient wave profile is linear. For this reason, we do not present here the lengthy derivation of the exact relation and perform further computations as if the incipient wave profile were linear. Similar to (26), we can write

$$\left(\frac{\partial \sigma_1}{\partial x}\right)^- - \left(\frac{\partial p}{\partial x}\right)^- \approx -\frac{s_0}{c_{\mathrm{d}1}}. \tag{49}$$

From the jump conditions, we have

$$\left[\!\left[\frac{\partial \sigma_1}{\partial x}\right]\!\right] = -\left(\frac{\partial \sigma_1}{\partial x}\right)^- = a_0 R_3, \tag{50}$$

$$\left[\!\left[\frac{\partial p}{\partial x}\right]\!\right] = -\left(\frac{\partial p}{\partial x}\right)^- = a_0 R_6, \tag{51}$$

where R_3, R_6 are given by (41), (42). Substituting (50), (51) into (49), we obtain

$$a_0 \approx -\frac{s_0}{R_1 \varrho_{\mathrm{s}} (c_{\mathrm{d}1}^2 - nc_{\mathrm{s}}^2)}. \tag{52}$$

As follows from inequalities (40), α_1 determined by (46) is positive unless $c_{\mathrm{f}}^2 = nc_{\mathrm{d1}}^2$. These two cases, $\alpha_1 > 0$ and $\alpha_1 = 0$, have to be considered separately.

Case $\alpha_1 > 0$. For $\alpha_1 > 0$, the critical distance is determined by (11). As the speed c_{d1} is taken to be positive, x_{c} must be positive as well. For given α_1, α_2, the value of x_{c} is determined by the boundary rate s_0 which is involved in (11) through a_0. The first condition for the critical distance to be positive is that the logarithm in (11) must be negative. The second condition is that the quantity under the logarithm must be positive. The two conditions together place a constraint on s_0. Under the assumption that the properties of the skeleton and the pore fluid in compression are such that $\beta_1 < 0$ and $\mathrm{d}K_{\mathrm{f}}/\mathrm{d}p > 0$, it can be found using (46), (47), (52) that the constraint on s_0 is $s_0 < s_0^*$, where

$$s_0^* = \frac{n\varrho_{\mathrm{s}} g(c_{\mathrm{d1}}^2 - nc_{\mathrm{s}}^2)(c_{\mathrm{f}}^2 - nc_{\mathrm{d1}}^2)^2}{k(1-n)^2 c_{\mathrm{f}}^2} \left[\frac{\beta_1 c_{\mathrm{s}}^2 (c_{\mathrm{d1}}^2 - c_{\mathrm{f}}^2)}{c_{\mathrm{d1}}^2 - c_{\mathrm{s}}^2} - \frac{\mathrm{d}K_{\mathrm{f}}}{\mathrm{d}p} \frac{(1-n)c_{\mathrm{d1}}^4}{n(c_{\mathrm{d1}}^2 - c_{\mathrm{f}}^2)} \right]^{-1}. \tag{53}$$

Since $s_0^* < 0$, the condition $s_0 < s_0^*$ means that the boundary loading must be compressive, and the magnitude of its rate must exceed $|s_0^*|$. The latter constitutes a qualitative difference with the undrained case where there is no restriction on the magnitude of the boundary rate for the formation of a shock front at a finite distance. Moreover, Eq. (53) shows that the minimum required rate tends to infinity as the permeability vanishes. This means that, for an arbitrarily high rate, no shock front is formed if the permeability is low enough. This result is in contradiction with the undrained case where a shock front is formed at any rate $s_0 < 0$. This inconsistency is explained as follows.

It can be shown that the characteristic wave speed c_{d1} is always larger than or equal to c_{u}, with the equality taking place in the exceptional case $\alpha_1 = 0$ discussed below. Since the permeability k appears in the right-hand side of system (31)–(36), the characteristic speed c_{d1} does not depend on k. As a consequence, at any finite permeability, however low, a weak discontinuity propagates with the speed c_{d1} and, in a time t, covers the distance $c_{\mathrm{d1}}t$, while the corresponding discontinuity in the undrained case propagates with the speed c_{u} and covers the distance $c_{\mathrm{u}}t$ which is shorter than $c_{\mathrm{d1}}t$. The wave profile in the drained case is such that, as k tends to zero, the leading part of the profile between $c_{\mathrm{u}}t$ and $c_{\mathrm{d1}}t$ becomes vanishingly small in magnitude. Thus, for low permeability in the drained case, the evolution equation for a weak discontinuity becomes misleading: this equation describes a weak discontinuity which belongs to the vanishing part of the wave profile rather than describing the part which propagates with c_{u} and is actually of interest.

Case $\alpha_1 = 0$. This exceptional case corresponds to the so-called dynamic compatibility [12–14] which is obtained if the parameters of the medium are such that

$$n\varrho_{\mathrm{f}}\kappa_1 = (1-n)(\varrho_{\mathrm{s}} - \varrho_{\mathrm{f}})K_{\mathrm{f}}. \tag{54}$$

Condition (54) leads to the equalities

$$c_{\mathrm{u}}^2 = c_{\mathrm{d1}}^2 = \frac{1}{n} c_{\mathrm{f}}^2. \tag{55}$$

Note also that the approximate relation (52) becomes exact in this case.

If (55) holds, α_1 given by (46) is zero, and the critical distance is determined by (10). It can be shown that the expression for the critical distance in the case of the dynamic compatibility reduces to (30) and is thus the same as in the undrained case, with no condition imposed on the magnitude of the boundary rate s_0.

5 Critical distances in a granular solid

In this Section we present numerical examples of critical distances in a saturated granular solid with particular constitutive behaviour of the solid skeleton and the pore fluid.

Assume that the initial stress state is hydrostatic, the constitutive behaviour of the skeleton in the vicinity of the initial state is isotropic, and the stiffness moduli depend on the mean effective pressure. For an isotropic solid with two independent stiffness moduli, the coefficients κ_2, κ_3 involved in the constitutive equations (14)–(16), (33)–(35) can be expressed through the coefficient κ_1 and the Poisson ratio ν:

$$\kappa_2 = \kappa_3 = \frac{\nu}{1-\nu}\kappa_1. \tag{56}$$

For granular solids such as sand or soil, the dependence of the stiffness on the confining pressure may be taken in the form of a power law [15–17]:

$$\kappa_1(\sigma) = \kappa_{10}\left(\frac{\sigma}{\sigma_0}\right)^m, \tag{57}$$

where $\sigma = (\sigma_1 + \sigma_2 + \sigma_3)/3$ is the mean effective stress, κ_{10} is a reference value of κ_1 at $\sigma = \sigma_0$, and m is an exponent lying typically in the range of 0.5–0.6.

The Poisson ratio ν for granular solids is an indeterminate quantity which depends on many factors, but fortunately its influence on the critical distance is insignificant. This can be shown by calculating β_1 in (48) with the use of (56) and (57):

$$\beta_1 = \frac{m\kappa_1(1+\nu)}{3\sigma(1-\nu)}. \tag{58}$$

The variation of ν, for instance, between 0.1 and 0.4 changes the ratio $(1+\nu)/(1-\nu)$ in (58) at most by a factor of 2. The same ratio appears in (23) when calculating β.

With the use of (57), the characteristic wave speed in a dry skeleton, c_s, given by (38) can be written as

$$c_s(\sigma) = c_{s0}\left(\frac{\sigma}{\sigma_0}\right)^{m/2}, \tag{59}$$

where c_{s0} is the value of c_s at $\sigma = \sigma_0$.

The pore fluid is assumed to consist of water with a small amount of free gas. The compressibility of such a fluid is strongly pressure dependent and differs substantially from the compressibility of pure water. Neglecting the surface tension between the liquid and the gaseous phases and taking the pressure in the liquid phase to be equal to the pressure in the gas, it can be shown (see, e.g. [18] or [17, Section 7.5.1]) that the compression modulus of a water–gas mixture is

$$K_f = (V_w + V_g)\left(\frac{V_w}{K_w} + \frac{V_g}{K_g}\right)^{-1} = \left(\frac{S_r}{K_w} + \frac{1-S_r}{K_g}\right)^{-1}, \tag{60}$$

where V_w and V_g are the volumes of the water and the gas in the mixture, K_w and K_g are the compression moduli of pure water and the gas, and $S_r = V_w/(V_w + V_g)$ is the degree of saturation.

For an ideal gas, $p_g V_g^\gamma = \text{const}$, where p_g is the absolute pressure of the gas (including the atmospheric pressure), $\gamma = 1$ for isothermal processes, and $\gamma = 1.4$ for adiabatic processes for air. This gives $K_g = \gamma p_g$.

As follows from (60), even a very small volume fraction of free gas drastically reduces the compression modulus of the fluid. For instance, the presence of 0.5 volume percent of gas with $K_g = 300$ kPa reduces the compression modulus of the water–gas mixture by a factor of 40 as compared with the modulus of pure water $K_w = 2.2$ GPa.

The calculation of the critical distance requires, besides K_f, knowledge of $\mathrm{d}K_f/\mathrm{d}p$. The quantities V_w, V_g and K_g in (60) are functions of p. Differentiating (60) with respect to p, we obtain after simple computations

$$\frac{\mathrm{d}K_f}{\mathrm{d}p} = \frac{K_f^2(1-S_r)\left[S_r(K_w-K_g)^2 + \gamma K_w^2\right]}{K_w^2 K_g^2} \approx \frac{K_f^2(1-S_r)(S_r+\gamma)}{K_g^2}, \tag{61}$$

where the last approximate expression is justified if $K_g \ll K_w$.

The parameters of the medium used in the calculations are given in Table 1. The wave speeds for this set of parameters are shown in Fig. 1 as functions of the gas content.

Figure 2 shows the quantity s_0^* determined by (53). Recall that $|s_0^*|$ gives the minimum required magnitude of the loading rate for the formation of a shock front. The value of s_0^* is inversely proportional to the permeability k and tends to minus infinity as the permeability vanishes, except for the case of the dynamic

Table 1 Parameters used in the calculations

c_{s0} (m/s)	σ_0 (kPa)	σ (kPa)	ν	m	K_g (kPa)	γ	K_w (GPa)	n	ϱ_s (kg/m^3)	ϱ_f (kg/m^3)
400	−200	−200	0.3	0.5	300	1.4	2.2	0.38	2,650	1,000

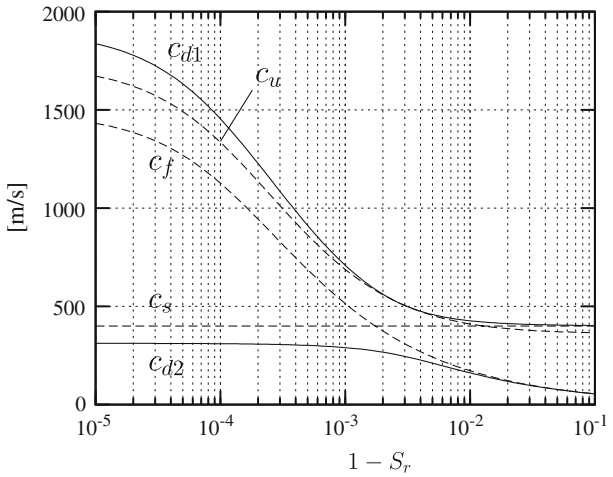

Fig. 1 Characteristic wave speeds as functions of the gas content

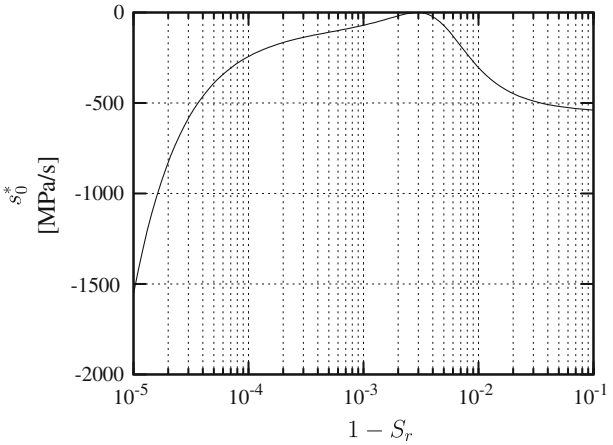

Fig. 2 Quantity s_0^* calculated with (53) for $k = 10^{-3}$ m/s

compatibility where s_0^* is always zero. As seen from Fig. 2, the dynamic compatibility in the present example occurs at a gas content of 3×10^{-3}. As the gas content tends to zero, s_0^* approaches a certain value. A feature of the asymptotic behaviour of s_0^* is that the approach is very slow: s_0^* continues to change markedly down to a gas content of 10^{-8}. The asymptotic value of s_0^* is of the order of -10^6 MPa/s and is much larger in magnitude than the values shown in Fig. 2.

Similarly to s_0^*, the quantities β, β_1 given by (23), (48) also exhibit slow asymptotic convergence to their limiting values as the gas content tends to zero. A consequence of the slow convergence of β, β_1 and s_0^* is the substantial change in the critical distance in the range of the gas content between 10^{-8} and 10^{-4}. This is illustrated in Figs. 3, 4 and 5 which show the critical distances for drained and undrained behaviour. The results are presented for the rate of boundary loading $s_0 = -10^4$ MPa/s relevant to blast loading.

Discuss first the undrained case for which the critical distance in Figs. 3, 4 and 5 is shown by the dashed line. Based on the shape of the curve, two characteristic ranges of the gas content can be distinguished. The first range covers the gas content between 10^{-4} and 10^{-1} and, in the context of soil mechanics, represents all physically meaningful values of the gas content for saturated soils. The critical distance in this range depends only slightly on the gas content and changes by a factor of two. This property is favourable for the theoretical prediction of the critical distance as it does not require exact knowledge of the degree of saturation within these specific limits. In the second range of the gas content from 10^{-4} down to 10^{-8}, the critical distance changes by three orders of magnitude before it reaches the asymptotic value. The extremely low values of the

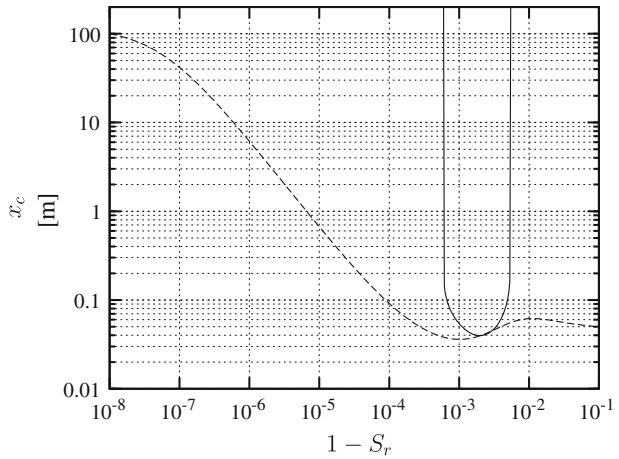

Fig. 3 Critical distances as functions of the gas content for the rate of boundary loading $s_0 = -10^4$ MPa/s. *Solid line* drained behaviour with $k = 10^{-5}$ m/s; *dashed line* undrained behaviour

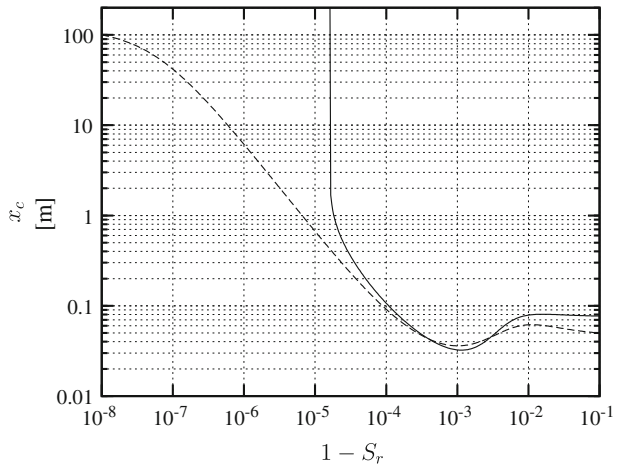

Fig. 4 The same as in Fig. 3 for $k = 10^{-4}$ m/s

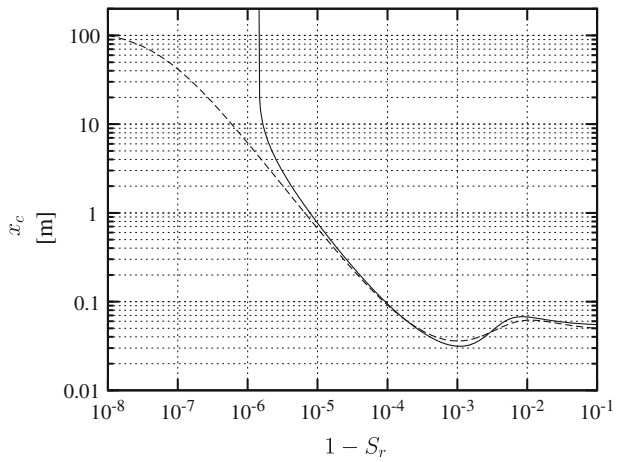

Fig. 5 The same as in Figs. 3 and 4 for $k = 10^{-3}$ m/s

gas content in the second range raise the questions of the physical feasibility of such small amounts of free gas in the pore fluid and the validity of Eqs. (60) and (61) in this range. However, even if such a small amount of gas can exist in a real solid, it cannot be homogeneous to give a definite value of the critical distance. From a practical point of view, this means the indeterminacy of the critical distance in the second range: if the gas content in a saturated solid is known to be lower than 10^{-4}, the critical distance will lie in a wide range (in the present example: between 0.1 and 100 m) and cannot be reliably predicted.

If the relative motion between the solid and the fluid phases is taken into account, both the critical distance and the minimum loading rate s_0^* depend on the permeability of the skeleton. The critical distance at low permeability is finite only in the vicinity of a certain value of the gas content corresponding to the dynamic compatibility (3×10^{-3} in the present example), see Fig. 3. As the permeability vanishes, the range of gas content where the critical distance is finite shrinks to zero. The reason why the drained model yields false results at low permeability has been discussed above: this model describes the discontinuity at the leading point of the front propagating with the speed c_{d1}. This part of the wave profile becomes vanishingly small in magnitude at low permeability, while the wave front as such propagates with the speed c_{u} which is less than c_{d1}.

As the permeability increases, the critical distance in the range of the gas content between 10^{-4} and 10^{-1} becomes close to the critical distance in the undrained model, see Figs. 4 and 5. Thus, in this range of the gas content, the undrained model may be used to calculate critical distances for both undrained and drained behaviour. The indeterminacy of the critical distance for the gas content below 10^{-4} remains valid in the drained case, with the difference that the upper limit of x_{c} may now be infinite if the applied loading rate s_0 is lower in magnitude than s_0^*.

6 Concluding remarks

The analysis of weak discontinuities in a fluid-saturated granular solid with pressure-dependent stiffness reveals that the evolution equation in the drained model with low permeability turns out to be misleading from the viewpoint of applications as it gives the correct critical distances only in the case of the dynamic compatibility. In general, the correct results are provided only by the undrained model. For high permeability, the critical distances in the drained model are close to those obtained with the undrained model, so that the latter may be used to calculate the critical distance for any value of the permeability.

Numerical calculations performed with particular constitutive relations show that, as the gas content varies between 10^{-4} and 10^{-1}, the critical distances vary insignificantly and differ by no more than a factor of two. In contrast, the critical distances for the gas content from 10^{-4} down to full saturation may differ by three orders of magnitude or more. In relation to real solids, this means that the critical distance is indeterminate if the gas content is below 10^{-4}.

Acknowledgments The study has been carried out within the framework of the project AISIS financed by the German Federal Ministry of Education and Research (BMBF).

References

1. Courant, R., Friedrichs, K.O.: Supersonic flow and shock waves. Springer, Berlin (1976)
2. Osinov, V.A.: On the formation of discontinuities of wave fronts in a saturated granular body. Continuum Mech. Thermodyn. **10**, 253–268 (1998)
3. Courant, R., Hilbert, D.: Methods of mathematical physics, vol. II, Partial differential equations. Interscience, New York (1965)
4. Whitham, G.B.: Linear and Nonlinear Waves. Wiley, New York (1974)
5. Boillat, G., Ruggeri, T.: On the evolution law of weak discontinuities for hyperbolic quasi-linear systems. Wave Motion **1**, 149–152 (1979)
6. Ruggeri, T.: Stability and discontinuity waves for symmetric hyperbolic systems. In: Jeffrey, A. (ed.) Nonlinear Wave Motion, pp. 148–161. Longman, London (1989)
7. Donato, A.: Nonlinear waves. In: Ames, W.F., Rogers, C. (eds.) Nonlinear Equations in the Applied Sciences, pp. 149–174. Academic Press, New York (1992)
8. Wilmanski, K.: Thermomechanics of Continua. Springer, Berlin (1998)
9. Wilmanski, K.: Critical time for acoustic waves in weakly nonlinear poroelastic materials. Continuum Mech. Thermodyn. **17**, 171–181 (2005)
10. Zienkiewicz, O.C., Chan, A.H.C., Pastor, M., Schrefler, B.A., Shiomi, T.: Computational geomechanics with special reference to earthquake engineering. Wiley, Chichester (1999)

11. Zienkiewicz, O.C., Shiomi, T.: Dynamic behaviour of saturated porous media: the generalized Biot formulation and its numerical solution. Int. J. Numer. Anal. Methods Geomech. **8**, 71–96 (1984)
12. Biot, M.A.: Theory of propagation of elastic waves in a fluid-saturated porous solid. I. Low-frequency range. J. Acoust. Soc. Am. **28**, 168–178 (1956)
13. Biot, M.A.: Mechanics of deformation and acoustic propagation in porous media. J. Appl. Phys. **33**, 1482–1498 (1962)
14. Simon, B.R., Zienkiewicz, O.C., Paul, D.K.: An analytical solution for the transient response of saturated porous elastic solids. Int. J. Numer. Anal. Methods Geomech. **8**, 381–398 (1984)
15. Hardin, B.O., Richart, F.E.: Elastic wave velocities in granular soils. J. Soil Mech. Found. Div., ASCE **89**, SM 1, 33–65 (1963)
16. Lambe, T.W., Whitman, R.V.: Soil Mechanics. Wiley, New York (1969)
17. Santamarina, J.C., Klein, K.A., Fam, M.A.: Soils and Waves. Wiley, Chichester (2001)
18. Osinov, V.A.: Cyclic shearing and liquefaction of soil under irregular loading: an incremental model for the dynamic earthquake-induced deformation. Soil Dyn. Earthq. Eng. **23**, 535–548 (2003)